Article

Structure and Dynamics of Solvated Sn(II) in Aqueous Solution: An ab Initio QM/MM MD Approach

Thomas S. Hofer, Andreas B. Pribil, Bernhard R. Randolf, and Bernd M. Rode

J. Am. Chem. Soc., **2005**, 127 (41), 14231-14238• DOI: 10.1021/ja052700f • Publication Date (Web): 22 September 2005

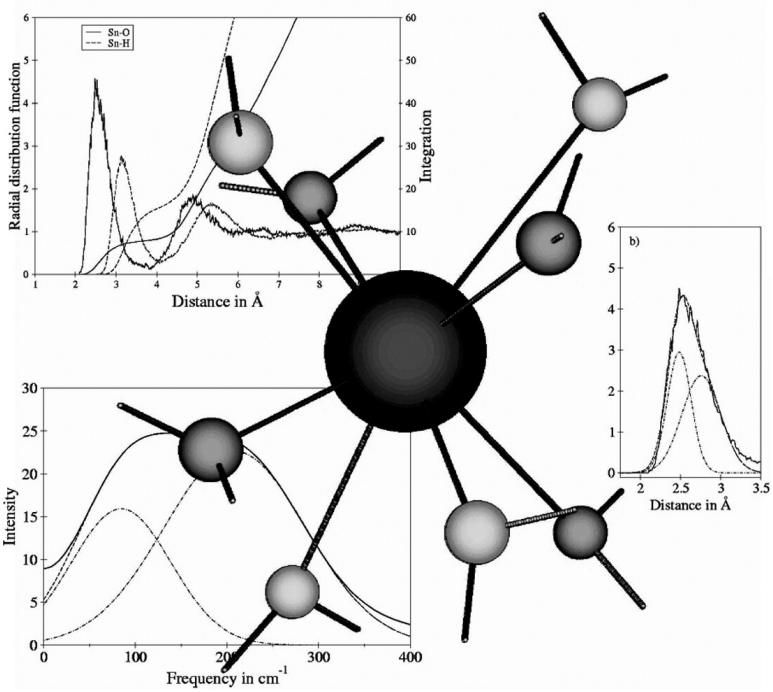

More About This Article

Additional resources and features associated with this article are available within the HTML version:

- Supporting Information
- Links to the 4 articles that cite this article, as of the time of this article download
- Access to high resolution figures
- Links to articles and content related to this article
- Copyright permission to reproduce figures and/or text from this article

View the Full Text HTML

J|A|C|S
ARTICLES
Published on Web 09/22/2005

Structure and Dynamics of Solvated Sn(II) in Aqueous Solution: An ab Initio QM/MM MD Approach

Thomas S. Hofer, Andreas B. Pribil, Bernhard R. Randolf, and Bernd M. Rode*

Contribution from the Theoretical Chemistry Division, Institute of General, Inorganic and Theoretical Chemistry University of Innsbruck, Innrain 52a, A-6020 Innsbruck, Austria

Received April 26, 2005; E-mail: Bernd.M.Rode@uibk.ac.at

Abstract: Structural and dynamical properties of the hydrated Sn(II) ion have been investigated by ab initio quantum mechanical/molecular mechanical (QM/MM) molecular dynamics (MD) simulations at double-ζ HF quantum mechanical level. The results indicate Sn(II)*aq* to be a rather peculiar, if not unique, case of a hydrated ion: four of its eight first-shell ligands do not take place in the otherwise frequent ligand-exchange processes, forming an approximately tetrahedral cage around the ion. The remaining ligands, however, exchange at a rate that is rather comparable to monovalent than divalent ions. This very surprising behavior of ligand exchange not yet observed in any previous simulation of over 30 hydrated metal ions is consistently confirmed by vibrational spectra, bond lengths, and a detailed analysis of the trajectories of the simulation.

1. Introduction

Tin is a very important basic material and plays an essential role in various industrial processes (for example coatings, various alloys as well as superconductors). Organotin compounds (especially trialkyl- and triaryltin) are used as bactericides and fungicides.[1] In marine environments tributyltin is commonly used as an antifouling agent;[1] however, there is concern over the environmental effects as these compounds cause severe problems to local wildlife.

In recent publications structure-breaking effects of the hydrated ions K(I),[2] Rb(I),[3] Cs(I),[4] Hg(II),[5]and Ba(II)[6] have been investigated with respect to structural and dynamical properties. However, a QM/MM MD simulation of Pb(II) revealed a very stable hydrate, with a nine-fold coordinated first shell.[7] No exchange event was observed within the simulation time of 25 ps. Just as lead is, tin is located in the fourth main group of the periodic table, and an interesting question, therefore, was whether a similar behavior would be observed in the case of Sn(II) in aqueous solution.

To our knowledge only few experimental investigations of $Sn(ClO_4)_2$ in aqueous solution have been carried out employing X-ray and EXAFS diffraction techniques. Two different Sn(II)−O bonds have been reported by Ohtaki,[8] one at about 2.3−2.35 Å, the other at about 2.8−2.9 Å. The average coordination number of the first shell has been given as ∼6. Yamaguchi et al. reported three to four water molecules in the immediate surrounding of Sn(II) which are strongly bound at 2.25−2.34 Å.[9] The molar ratios of the solutions employed had values of 16.8 and 12.0, respectively. It has to be considered that in these highly concentrated solutions too few ligand molecules are available to fully and properly hydrate the ions and to form a complete first, much less a second hydration shell, with an appropriate number of bulk molecules to investigate ligand-exchange events. Hence, these data do not reflect the situation in dilute solution and have to be considered as guidelines only.

Therefore, the hydration structure of Sn(II) still remains a very interesting challenge for both theory and experiment. Several recent investigations of solvated ions have proven that MD simulations are suitable tools to obtain realistic data of solvation structures,[10] if the QM/MM approach is employed to include many-body effects, using at least double-ζ basis sets for the Hartree−Fock ab initio treatment of the quantum mechanical part.

Information on the dynamic behavior of weakly hydrated ions is still limited. Various techniques (NMR, incoherent quasi-elastic neutron scattering (IQENS) and other relaxation techniques) have been utilized in studies on dynamic properties of hydrated ions and rates of substitution of water molecules in the first and second hydration shell. The experimentally estimated rate constant for first-shell water exchange of Sn(II) obtained by IQENS is 10^9-10^{10} s^{-1}, which is at the methodical time-range limit of $\geq 10^{-9}$ s for this method.

Previous investigations of the Cs(I) ion in aqueous solution[4] have yielded a mean ligand residence time (MRT) of ∼2 ps, which is 2 orders of magnitude smaller than the experimental

(1) da Silva, J. J. R. F.; Williams, R. J. P. *The Biological Chemistry of Life*; Clarendon Press: Oxford, 1991.
(2) Tongraar, A.; Liedl, K. R.; Rode, B. M. *J. Phys. Chem. A* **1998**, *102*, 10340−10347.
(3) Thomas S. Hofer, B. R. R.; Rode, B. M. *J. Comput. Chem.* **2005**, *26*, 949.
(4) Schwenk, C. F.; Hofer, T. S.; Rode, B. M. *J. Phys. Chem. A* **2004**, *108*, 1509.
(5) Kritayakornupong, C.; Plankensteiner, K.; Rode, B. M. *Chem. Phys. Lett.* **2003**, *371*, 438.
(6) Hofer, T. S.; Randolf, B. R.; Rode, B. M. *Chem. Phys.* **2005**, *312*, 81.
(7) Hofer, T. S.; Rode, B. M. *J. Phys. Chem.* **2004**, *121*, 6406.
(8) Ohtaki, H.; Radnai, T. *Chem. Rev.* **1993**, *93*, 1157.
(9) Yamaguchi, T.; Lindqvist, O.; Claeson, T.; Boyce, J. B. *Chem. Phys. Lett.* **1982**, *93*, 528.
(10) Schwenk, C. F.; Tongraar, A.; Rode, B. M. *J. Mol. Liquids* **2004**, *110*, 105.

Table 1. Average Binding Energies in kcal/mol for $[Sn(H_2O)_n]^{2+}$ Clusters Obtained from HF, CCSD, QCISD, MP4-SDQ, MP2, and B3LYP Calculations

	E_{bond} in kcal/mol					
n	HF	CCSD	QCISD	MP4–SDQ	MP2	B3-LYP
1	−62.7	−65.2	−65.4	−65.7	−67.8	−72.8
2	−51.2	−54.2	−54.3	−54.5	−55.9	−59.5
3	−53.5	−55.4	−55.5	−55.7	−57.5	−60.5
4	−46.7	−48.7	−48.8	−49.0	−50.5	−52.6
6	−37.2	−39.3	−39.4	−39.6	−40.6	−42.0
8	−31.7	−33.8	−33.8	−34.0	−34.7	−35.2

Table 2. Average Sn−O Distances in Å for $[Sn(H_2O)_n]^{2+}$ Clusters Obtained from HF, CC-D, MP4-SDQ, QCISD, MP2, and B3LYP Calculations

	r_{Sn-O} in Å					
n	HF	CCSD	QCISD	MP4–SPD	MP-2	B3-LYP
1	2.23	2.23	2.24	2.23	2.23	2.21
2	2.41	2.38	2.38	2.38	2.38	2.36
3	2.29	2.29	2.29	2.29	2.28	2.27
4	2.39	2.39	2.39	2.39	2.38	2.36
6	2.62	2.59	2.59	2.59	2.57	2.56
8	2.72	2.69	2.69	2.69	2.66	2.65

Table 3. Basis Set Superposition Error According to Boys−Bernardi Procedure for Sn(II)−H_2O in HF, CCSD, QCISD, MP4-SDQ, MP2, and B3LYP Calculations

	BSSE in kcal/mol				
HF	CC-D	QCISD	MP4–SDQ	MP2	B3-LYP
0.7	1.3	1.4	1.4	1.4	1.5

estimation of ∼200 ps. A time step of 0.2 fs used in MD simulations allows the prediction of dynamical processes even in the femtosecond range. Ab initio QM/MM MD simulations of several similar systems, including pure water, have yielded adequate MRTs, proving the suitability of this methodology to describe ultrafast dynamics.[11]

The objective of this work was to obtain an accurate description of the Sn(II) hydrate structure in aqueous solution and of the dynamical properties of this hydrate.

2. Methods

One of the most important criteria of a QM/MM simulation is the choice of a proper basis set, as it will be a compromise between computational demand and accuracy of results. The basis set for heavy ions should also include an effective core potential (ECP), which has been corrected to take into account relativistic effects. The number of literature-available basis sets is quite limited in the case of tin. The SBKJC VDZ ECP basis set was chosen for tin,[12] as it includes a relativistically corrected ECP and proved most stable in sampling of the Sn(II)−H_2O energy surface. For hydrogen and oxygen DZP basis sets[13] were employed.

Concerning the level of theory for the QM region, either DFT or ab initio HF are manageable, considering the amount of necessary computational effort. In recent investigations of similar ionic systems, results of HF calculations were in good agreement with experimental data, whereas simple DFT methods such as BP86 and RIDFT[4,14,15] seemed to fail, and even the more sophisticated hybrid B3-LYP functional sometimes yielded deviating descriptions,[4,14,15] or at best, a proper description of the system without any time-saving effect.

To estimate whether our method of choice is reliable, geometry optimizations of $[Sn(H_2O)_n]^{2+}$ clusters were performed employing different levels of theory utilizing the programm package GAUSSIAN03.[16] Tables 1 and 2 list the average binding energies and Sn−O distances calculated for different cluster sizes $[Sn(H_2O)_n]^{2+}$ ($n = 1-8$) at Hartree−Fock, MP4-SDQ, CCSD, QCISD, MP2, and B3-LYP level using DZP basis sets for hydrogen and oxygen[13] and the SBKJC VDZ ECP basis set for tin.[12] The results indicate both the possible role of electron correlation and many-body effects to be expected in the simulation. Further, they are helpful to decide whether the B3-LYP or the ab initio HF formalism produce more accurate data compared to the correlated methods MP4-SDQ, QCISD, and CCSD.

The relative scale lists the average binding energies from the highest to the lowest values of E_{bond}:

$$HF > CCSD \approx QCISD > MP4\text{-}SDQ > MP2 > B3\text{-}LYP$$

In general, MP4-SDQ, QCISD, and CCSD yield the same result; the deviation of the values are in the order of 0.2 kcal/mol and less. Comparing HF and B3-LYP with MP4-SDQ, QCISD, and CCSD the difference in the energy is on the order of ∼2.0 kcal/mol, respectively. However, the deviations are in opposite directions: the HF energy is above the energy of the correlated methods due to the neglect of electron correlation, whereas the binding energies in the B3-LYP case are lower, most probably due to an overestimation of correlation influence as also encountered in the MP2 calculations.

Comparing the average binding energies for varying ligand number with those of the ions Cs(I)[4] and Ca(II)[14] it can be seen that many-body effects have some noticeable influence. Therefore, the inclusion of a three-body potential will improve the description of the MM region of this system. Another possibility to determine the suitability of a method are the structural properties, especially the ion−oxygen bond length. The values obtained from the different calculations are in good agreement except for B3-LYP which shows in all cases a smaller bond length than all other methods.

Finally, an estimation of the influence of the basis set superposition error (BSSE) was performed for Sn(II) monohydrates (Table 3).

It can be seen that the BSSE error of the ab initio HF method makes it more favorable over the B3-LYP formalism. As one of the main interests of this simulation are structural properties of the Sn(II) hydrate, the ab initio HF-SCF formalism was clearly preferable to describe the QM region in the simulation. According to the test calculations it can also be concluded that the effects of electron correlation and BSSE should have only a minor influence on the QM/MM simulation quality.

The pair potential for the Sn(II) water interaction was newly constructed, applying DZP basis sets for hydrogen and oxygen[13] and the SBKJC VDZ ECP basis set for Sn(II). Six thousand one hundred and thirty Hartree−Fock interaction energy points calculated by the TURBOMOLE 5.5 program[17−20] were fitted to an analytical form by a least-squares error minimization using the Levenberg−Marquardt algorithm.

$$E_{2bd} = \frac{q_O q_{Sn}^{II}}{r} + \frac{A_O}{r^5} + \frac{B_O}{r^7} + \frac{C_O}{r^{11}} + \frac{D_O}{r^{12}} + \sum_{i=1}^{2}\left(\frac{q_H q_{Sn}^{II}}{r_i} + \frac{A_H}{r_i^4} + \frac{B_H}{r_i^6} + \frac{C_H}{r_i^7} + \frac{D_H}{r_i^{12}}\right) \quad (1)$$

(11) Hofer, T. S.; Tran, H. T.; Schwenk, C. F.; Rode, B. M. *J. Comput. Chem.* **2004**, *25*, 211.
(12) Stevens, W. J.; Krauss, M.; Bash, H.; Jasien, P. G. *Can. J. Chem.* **1992**, *70*, 612.
(13) Dunning, T. H., Jr. *J. Chem. Phys.* **1970**, *53*, 2823.
(14) Schwenk, C. F.; Löffler, H. H.; Rode, B. M. *J. Chem. Phys.* **2001**, *115*, 10808.
(15) Schwenk, C. F.; Rode, B. M. *J. Chem. Phys.* **2003**, *119*, 9523.
(16) Frisch, M. J. et al. 2004.
(17) Ahlrichs, R.; Bär, M.; Häser, M.; Horn, H.; Kölmel, C. *Chem. Phys. Lett.* **1989**, *162*, 165.

Table 4. Optimized Parameters for Sn−O and Sn−H Two-Body Interactions in Å^n·kcal/mol[a]

	A	B	C	D
Sn−O	−7867.90	43232.06	−431875.82	478191.54
Sn−H	−587.93	9697.18	−12915.81	9601.18

[a] n is according to formula 1.

Table 5. Optimized Parameters for $[Sn(H_2O)_2]^{2+}$ Three-body Interaction

A	*B*	*C*
0.9929528 kcal/mol	1.8350491 Å^{-1}	−1.4383524 Å^{-1}

The values of −0.65966 and 0.32983 were adopted for q_O and q_H in accordance with the charges of the flexible BJH-CF2 water model.[21,22] The experimental gas-phase geometry of water was fixed (O−H distance of 0.9601 Å and H−O−H angle of 104.47°). The value of the global energy minimum is −62.5 kcal/mol at a distance of 2.237 Å and the root-mean-square deviation (rmsd) of the fitted function was 1.1 kcal/mol. The fitting parameters *A*, *B*, *C*, and *D* for oxygen and hydrogen are listed in Table 4.

As optimizations of the Sn(II) water clusters had revealed that many-body interactions play a major role, a potential was constructed to correct the two body potential with respect to three-body terms. More than 24000 interaction points of the Sn(II)$(H_2O)_2$ hypersurface were calculated by the TURBOMOLE 5.5 program[17−20] and fitted to an analytical form by a least-squares error minimization, using again the Levenberg−Marquardt algorithm.

$$E_{3bd} = Ae^{Br_{12}}e^{Br_{13}}e^{Cr_{23}}(r_{cut} - r_{12})^2(r_{cut} - r_{23})^2 \qquad (2)$$

r_{12} and r_{13} are the ion−oxygen distances for water molecules one and two, respectively, r_{23} is the oxygen−oxygen distance between both water molecules. The cutoff radius r_{cut} is set to 6.0 Å. The optimized parameters *A*, *B*, and *C* are listed in Table 5.

The QM/MM technique[23−25] used in this work divides the system into a part treated by means of the respective quantum mechanical technique (QM), containing the ion and the full first hydration shell, while the rest of the system is described by means of classical molecular mechanics (MM). This treatment does not allow an analytical evaluation of the energy expression as molecules contribute different energy values depending on their location in the system (either QM or MM region). Thus, a transition of molecules from QM to MM region or vice versa means a considerable change in the total energy which makes a treatment depending on energy values (e.g., Monte Carlo simulations, free energy calculations, etc.) more complex. The ONIOM-XS method[26,27] recently introduced by Kerdcharoen and Morokuma treats molecules transiting from QM to MM at both levels of theory in order to gain a steady energy transition. In this case every time a molecule is located in the transition region between QM and MM region, two quantum mechanical calculations are necessary per step, which can extend the computational effort considerably. For systems experiencing a large number of ligand-exchange reactions (e.g. structure-breaking ions such as Rb(I)[3] and Cs(I),[4] extended QM/MM simulations including first and second hydration shells) the computational effort would be almost doubled. The formalism used in this work only depends on forces, for which a simple smoothing procedure is sufficient to consider the different regions and transitions between them thus keeping the computational effort at a less costly level.

The QM/MM MD protocol employed in the present work is based on the following subtractive force expression:

$$F_{tot} = F_{MM}^{sys} + (F_{QM}^{QM} - F_{QM}^{MM}) \times S(r) \qquad (3)$$

where F_{tot} is the total force acting on a particle, F_{MM}^{sys} is the MM force of the whole system, F_{QM}^{QM} is the QM force in the QM region, and F_{QM}^{MM} is the MM force in the QM region. F_{QM}^{MM} accounts for the coupling between QM and MM region. The QM/MM MD program allows water molecules to leave and enter the QM region as needed. To ensure a continuous change of forces, a smoothing function $S(r)$ is applied between the radii r_0 and r_1:

$$S(r) = 1, \quad \text{for } r \le r_1$$

$$S(r) = \frac{(r_0^2 - r^2)^2(r_0^2 + 2r^2 - 3r_1^2)}{(r_0^2 - r_1^2)^3}, \quad \text{for } r_1 < r \le r_0$$

$$S(r) = 0, \quad \text{for } r > r_0$$

The simulation protocol was similar to that of previous investigations.[28,29] The simulation was carried out in the canonical *NVT* ensemble, consisting of one Sn(II) ion and 499 water molecules in a cubic box of 24.8 Å. The simulation temperature of 298 K was kept constant using the Berendsen algorithm,[30] and the bath relaxation time was set to 0.1 ps. The density of the system was assumed to be 0.997 g/cm^3, which is the density of pure water at the simulation temperature. The reaction field method[31] was employed to correct the cutoff of long-range electrostatic interactions. The Newtonian equations of motion were treated by a general predictor-corrector algorithm, and a time step of 0.2 fs was chosen, since the BJH-CF2 water model[21,22] allows explicit hydrogen movements.

A classical pair potential molecular dynamics simulation was performed first for 100 ps, starting from a random configuration. With this equilibrated system another molecular dynamics simulation with two- and three-body potentials was performed for another 100 ps. The combined QM/MM molecular dynamics simulation, in which the ion and its full first hydration shell were included into the QM region (QM diameter of 8.4 Å), started from the equilibrium configuration resulting from the classical simulation. After 2 ps of reequilibration another 30 ps of sampling was performed. The net calculation time for the QM/MM MD simulation was about 7.5 months on four 2.4 GHz Intel processors.

Besides structural properties such as radial distribution functions, coordination numbers, and various angle distributions, dynamical properties such as water-exchange rate constants, mean residence times of ligand molecules, vibrational and rotational motions, and the ion−oxygen frequency were evaluated. Velocity autocorrelation functions (VACFs) *C(t)* give direct insight into the dynamics of a fluid system as the time integrals are related to macroscopic transport coefficients, and their Fourier transformations are related to vibrational spectra.

$$C(t) = \frac{\sum_i^{N_t}\sum_j^{N} \vec{v}_j(t_i)\,\vec{v}_j(t_i + t)}{N_t N \sum_i^{N_t}\sum_j^{N\,\vec{v}_j} (t_i)\vec{v}_j(t_i)} \qquad (5)$$

(18) Brode, S.; Horn, H.; Ehrig, M.; Moldrup, D.; Rice, J. E.; Ahlrichs, R. *J. Comput. Chem.* **1993**, *14*, 1142.
(19) Ahlrichs, R.; von Arnim, M. In *Methods and Techniques in Computational Chemistry: METECC-95*; Clementi, E., Corongiu, G., Eds.; STEF, Cagliari, 1995; Chapter 13, pp 509−554.
(20) von Arnim, M.; Ahlrichs, R. *J. Comput. Chem.* **1998**, *19*, 1746.
(21) Stillinger, F. H.; Rahman, A. *J. Chem. Phys.* **1978**, *68*, 666.
(22) Bopp, P.; Janscó, G.; Heinzinger, K. *Chem. Phys. Lett.* **1983**, *98*, 129.
(23) Gao, J. In *Reviews in Computational Chemistry*, Lipkowitz, K. B., Boyd, D. B., Eds.; VCH Publishers: New York, 1996; Vol. 7, Chapter 3, pp 119−185.
(24) Gao, J. *Acc. Chem. Res.* **1996**, *29*, 298.
(25) Bakowies, D.; Thiel, W. *J. Phys. Chem.* **1996**, *100*, 10580.
(26) Kerdcharoen, T.; Morokuma, K. *Chem. Phys. Lett.* **2002**, *355*, 257.
(27) Kerdcharoen, T.; Morokuma, K. *J. Chem. Phys.* **2003**, *118*, 8856.
(28) Löffler, H. H.; Rode, B. M. *J. Chem. Phys.* **2002**, *117*, 110.
(29) Inada, Y.; Löffler, H. H.; Rode, B. M. *Chem. Phys. Lett.* **2002**, *358*, 449.

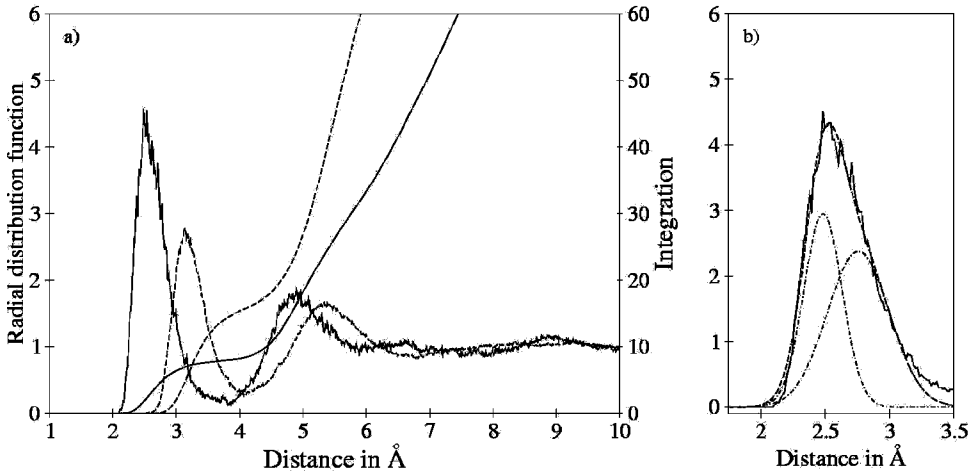

Figure 1. (a) Sn−O (solid line) and Sn−H (dashed line) radial distribution functions and their running integration numbers. (b) Linear combination of Gaussian functions fitted to the first-shell peak of the Sn−O RDF.

where N is the number of particles, N_t is the number of time origins t_i, and $\vec{v}_j$ denotes a certain velocity component of particle j. A correlation length of 2.0 ps was used to obtain the power spectra with 2000 (QM/MM) averaged time origins. The ion−water vibrational frequency was then computed using the approximative normal coordinate analysis.[32] The standard scaling factor of 0.89[33,34] was applied to scale the computed HF frequencies in order to make them directly comparable with experimental data.

A large number of second-shell and several first-shell exchange processes were observed within the simulation time of 30 ps. In a previous investigation[11] we have compared two different evaluation methods for MRTs, namely the "direct" method, accounting for all actually incoming and outgoing ligands, and the procedure suggested by Impey et al.,[35] based on a "survival function". This work has shown that the usage of a full accounting of all ligand movements ("direct" method) is advantageous and that the most appropriate time span to record a ligand displacement from its original coordination sphere as an exchange process is 0.5 ps.[11] This time interval also corresponds to the average lifetime of a hydrogen bond in the solvent.[36]

Simulation data can provide further information concerning the lability of the hydration shell, measurable by the number and "sustainability" of ligand-exchange processes.[11] It is possible to measure the number of exchange events leading to a longer-lasting change in the hydration structure by comparing the number of transitions through a shell boundary (N_{ex}^{0}) to the number of changes persisting after 0.5 ps ($N_{ex}^{0.5}$), thus defining a sustainability coefficient:[11]

$$S_{ex} = \frac{N_{ex}^{0.5}}{N_{ex}^{0}}$$

Its inverse ($1/S_{ex}$) accounts for how many border-crossing attempts are needed to produce one longer-lasting change in the hydration structure of an individual ion.[11]

Results and Discussion

3.1. Structure. The Sn−O radial distribution function reveals two well-defined hydration shells (cf. Figure 1a); a third shell cannot be distinguished from the bulk.

The RDF shape indicates a rather well-defined but flexible first shell with its maximum located at 2.5 Å. The peak shows a significant tailing toward the second shell, and despite considerable noise, a slight shoulder can be distinguished at about 2.65 Å. To gain further information concerning the first shell a linear combination of two Gaussian functions was fitted to the first-shell peak (cf. Figure 1b). Although this approach is very simple, two distinct functions can be observed peaking at ∼2.45 and ∼2.75 Å, thus indicating that two different bond lengths are favored within the first shell. No further structural information can be gained, if the number of Gaussian functions is increased to three or more, confirming the assumption of only two different binding states.

This finding agrees with the data presented by Ohtaki[8] who reported two distinct bond lengths at 2.3−2.35 Å and 2.8−2.9 Å. The single bond length reported by Yamaguchi and coworkers is 2.25−2.34 Å. The deviations between these studies and the results of the QM/MM MD simulation could be explained by association effects and polarization within the highly concentrated solution employed for the experimental investigations. On the other hand the Gaussian fit is a very simple approach to distinguish bond lengths, and therefore, a large standard deviation has to be assumed.

A similar QM/MM MD simulation of hydrated Pb(II) has also shown the presence of several species within the first shell.[7]

By its distance to the baseline, the minimum between first and second hydration shell clearly indicates frequent ligand exchanges. The differentiated as well as the integrated RDF makes it possible to locate the intershell borderline within ±0.05 Å at 3.8 Å. Integration of the RDF yields an average coordination number of ∼8 for the first shell, which suggests 8 to be the most populated coordination number.

The broad second shell shows a maximum at 4.9 Å. The border between second shell and bulk, however, is not well defined. Again, differentiation and integration of the RDF helps to define the borderline of the second shell within ±0.05 Å at 5.9 Å. The average coordination number of the second shell obtained via integration is ∼24.

The Sn−H radial distribution function shows two clearly defined peaks separated by a noticeable minimum. The first shell of hydrogens has its maximum at 3.1 Å, and the borderline between first and second shell is located at 4.1 Å. An average

(30) Berendsen, H. J. C.; Postma, J. P. M.; van Gunsteren, W. F.; DiNola, A.; Haak, J. R. *J. Phys. Chem.* **1984**, *81*, 3684.
(31) Adams, D. J.; Adams, E. M.; Hills, G. *J. Mol. Phys.* **1979**, *38*, 387.
(32) Bopp, P. *Chem. Phys.* **1986**, *106*(205−212).
(33) Scott, A. P.; Radom, L. *J. Phys. Chem.* **1996**, *100*, 16502.
(34) DeFrees, D. J.; McLean, A. D. *J. Chem. Phys.* **1985**, *82*, 333.
(35) Impey, R. W.; Madden, P. A.; McDonald, I. R. *J. Phys. Chem.* **1983**, *87*, 7, 5071.
(36) Lock, A. J.; Woutersen, S.; Bakker, H. J. *Femtochemistry and Femtobiology*: World Scientific: River Edge, NJ, 2001.

Table 6. Maxima r_M and Minima r_m of the Radial Distribution Functions in Å and Average Coordination Numbers of the Respective Shells

	structure					
	r_{M1}	r_{m1}	r_{M2}	r_{M2}	$CN_{av,1}$	$CN_{av,2}$
Sn−O	2.53[a]	3.82	4.90	5.88	7.99	23.6
Sn−H	3.13	4.06	5.34	6.77	15.6	71.8

[a] average; two distinct bond distances have been identified at 2.45 and 2.75 Å

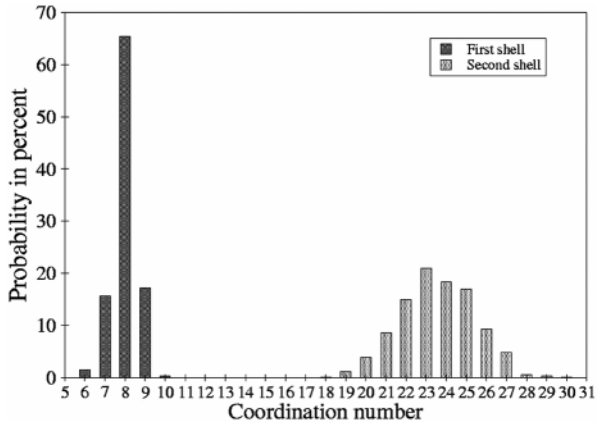

Figure 2. Coordination number distributions of the first and second hydration shell of Sn(II) in aqueous solution.

coordination number for the first shell of 15.6 is obtained. This value does not exactly correspond to the coordination number deduced from the Sn−O radial distribution function and thus suggests a high degree of mobility between the first and second shells (Table 6).

The second shell of the Sn−H RDF has its maximum at 5.6 Å; the borderline between second shell and bulk was located by differentiation and integration of the RDF within ±0.1 Å at 6.8 Å, thus yielding a coordination number of ∼72. Again, this value does not correspond to the coordination number obtained from the Sn−O RDF and points once more toward a very mobile structure associated with rapid ligand movements between second shell and bulk.

The coordination numbers (cf. Table 3.1) obtained from the RDFs are only average values. To get more information concerning the actual coordination numbers in first and second hydration shell a Sn−O coordination number distribution (CND) plot was generated (cf. Figure 2) by defining the shell borders according to the Sn−O RDF.

The distribution of the coordination numbers in the first shell varies from 6 to 10. The most probable configuration occurring with a probability of 65% contains eight ligands as concluded from the Sn−O radial distribution function, followed by coordination numbers 9 and 7 which occur with a probability of 17 and 16%, respectively. The probability of the other occurring coordination numbers is less than 2%.

In the second shell, a very broad distribution of the coordination numbers is observed, varying over a wide range from 18 to 30. The most probable number of ligands is 23, but its probability is only 23%; consequently, a distinct second-shell coordination number cannot be defined. The value ∼24 obtained from RDF running integration seems to be a reasonable average for the second shell of the Sn(II) ion, however.

These wide coordination number distributions also indicate the occurrence of ligand-exchange reactions between the first and second hydration shells as well as between the second shell and bulk.

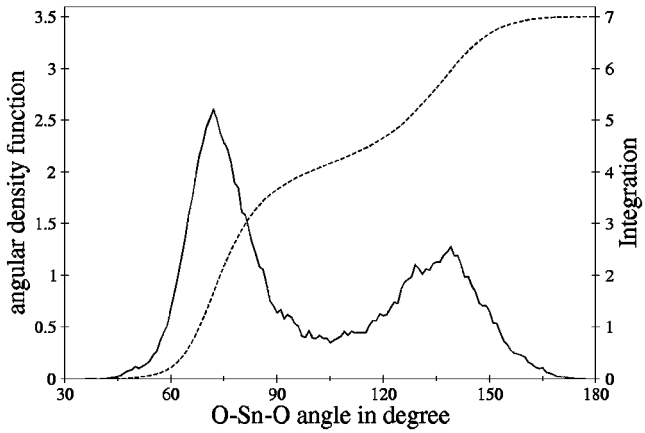

Figure 3. Angular distribution function of the O−Sn−O angle in the first hydration shell.

The hydration structure can be further discussed on the basis of angular distribution functions (ADF). Figure 3 shows the distribution of the oxygen−tin−oxyygen angle in the first shell. Two broad peaks are separated by a minimum point toward a flexible structure within the first shell. The distribution function is starting at ∼36° and rises quickly to the first maximum at 72°. The second maximum is situated at ∼139°. The ADF reaches zero again at 180°, with a significant tailing toward large angles. The minimum between the two peaks is located at approximately 105°.

The relative orientation of the water ligands gives further insight into the hydrate's structure. Therefore, two different angles were defined: θ as the angle between the O−Sn vector and the vector resulting from the sum of the O−H vectors. The tilt angle is the angle between the Sn−O vector and the plane defined by the O−H vectors. Tilt and θ angle distributions are depicted in Figure 4a,b.

The distribution of the tilt angle shows an extraordinary broad peak compared to those of other divalent ions. Its maximum is located at 0°, and the distibution reaches zero at ±90°. It can be seen that the half-width is very broad and covers a region of about ±45°, another indication of a high flexibility of ligand arrangements within the first hydration shell. The θ angle peaks at ∼155° with significant tailing toward ∼75°, showing a high variability of ligand orientation within the first shell compared to other hydrated divalent cations such as Ca(II),[14] Cu(II),[37] Co(II)[38] or even the labile Hg(II).[5] This distribution of the θ angle rather corresponds to systems such as hydrated Au(I)[39] or Ag(I)[40] and may be based on the large ionic radius of Sn(II) and the low surface charge density compared to those of the aforementioned divalent cations. A similar behavior has also been observed in the case of hydrated Pb(II).[7]

3.2. Dynamics. 3.2.1. Rotational and Vibrational Motions. The scaled power spectrum of the Sn(II)−O vibrational mode in the first hydration shell is displayed in Figure 5. The peak shows a broad plateau indicating that more than one bond length

(37) Schwenk, C. F.; Rode, B. M. *ChemPhysChem* **2003**, *4*, 931.
(38) Armunanto, R.; Schwenk, C. F.; Setiaji, A. H.; Rode, B. M. *Chem. Phys.* **2003**, *295*, 63.
(39) Armunanto, R.; Schwenk, C. F.; Tran, H. T.; Rode, B. M. *J. Am. Chem. Soc.* **2004**, *126*, 2582.
(40) Armunanto, R.; Schwenk, C. F.; Rode, B. M. *J. Phys. Chem. A* **2003**, *107*, 3132.

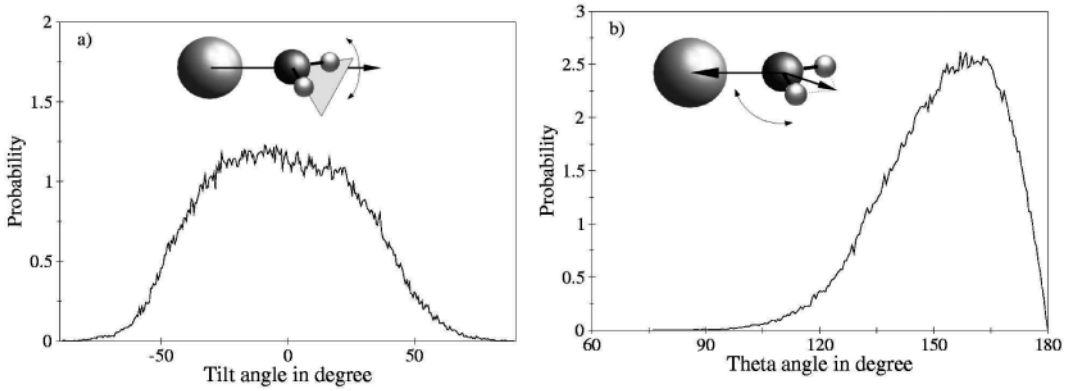

Figure 4. (a) Tilt angle and (b) θ angle distributions (for definitions see main text) of the Sn−H_2O geometry.

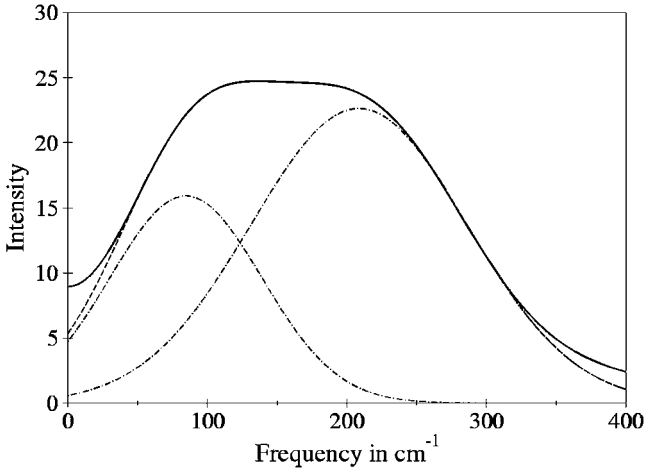

Figure 5. Power spectrum of the Sn(II)−O stretching mode in the first hydration shell (solid line). The fitted spectrum is shown as dashed line, the Gaussian functions are depicted as dashed−dotted lines.

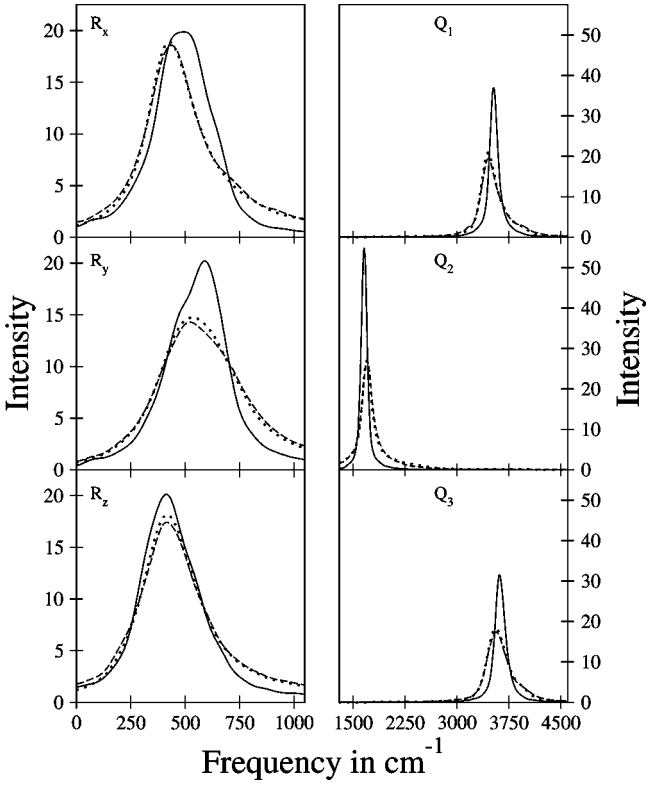

Figure 6. Power spectra in cm^{-1} of vibrational and librational motions of the water molecules in the first (solid line) and second (dashed line) hydration shell as well as in the bulk (dotted line).

is preferred as already deduced from the Sn−O RDF. Two distinct Gaussian functions could be fitted to the spectra, one peaking at 85 the other one at 208 cm^{-1}, with corresponding force constants of 6.0 and 36.1 N/m, respectively. As in the case of the fist shell peak of the Sn(II)−O RDF an increasing number of Gaussian functions does not improve the fitting. The resulting two distinct wavenumbers are consistent with the results of two distinct Sn(II)−O bond length discussed above. The higher value of 208 cm^{-1} is in good agreement with previous investigations of labile hydrates. The scaled average frequency of the Pb(II)−O stretching motion is 217 cm^{-1}, the corresponding force constant is 37.4 N/m proving weak ligand bonding in the first shell, comparable to Ba(II)[6] whose ion−oxygen stretching motion shows a frequency of 200 cm^{-1} and a force constant of 33.8 N/m, whereas the corresponding frequencies of other divalent ions such as Ca(II),[41] Hg(II),[5] Co(II),[38] or Fe(II)[42] are significantly higher, namely 260, 271, 305, and 313 cm^{-1}, respectively, with corresponding force constants of 46, 64, 69, and 72 N/m.

The lower value of the force constant of 6.0 N/m is on the same order of magnitude as the values obtained from QM/MM MD simulations of the ions Rb(I) and Cs(I),[4] which show frequencies of 106 and 100 cm^{-1} and force constants of 8.9 and 8.5 N/m, respectively. These hydrates are known for their structure-breaking properties and exchange their ligands within the picosecond scale. It can be concluded, therefore, that this is also the case for some ligands in the first hydration shell of Sn(II).

The spectra of the vibrational motions of water molecules Q_1, Q_2, Q_3 in the first and the second shell as well as in the bulk are displayed in Figure 6, the corresponding frequencies are listed in Table 7. The frequencies in the bulk are consistent with previously obtained data from MD simulations[32,44] and experimental values.[43] The bending frequency of the first shell is slightly red-shifted compared to the bulk, whereas the stretching frequencies are blue-shifted. This is consistent with investigations of other hydrated ions.[10] The second-shell frequencies are corresponding to the values obtained for bulk

(41) Schwenk, C. F.; Löffler, H. H.; Rode, B. M. *Chem. Phys. Lett.* **2001**, *349*, 99.
(42) Remsungnen, T.; Rode, B. M. *Chem. Phys. Lett.* **2003**, *367*, 586.
(43) Murphy, W. F.; Bernstein, H. J. *J. Phys. Chem.* **1972**, *76*, 1147.
(44) Spohr, E.; Pálinkás, G.; Heinzinger, K.; Bopp, P.; Probst, M. M. *J. Phys. Chem.* **1988**, *92*, 6754.

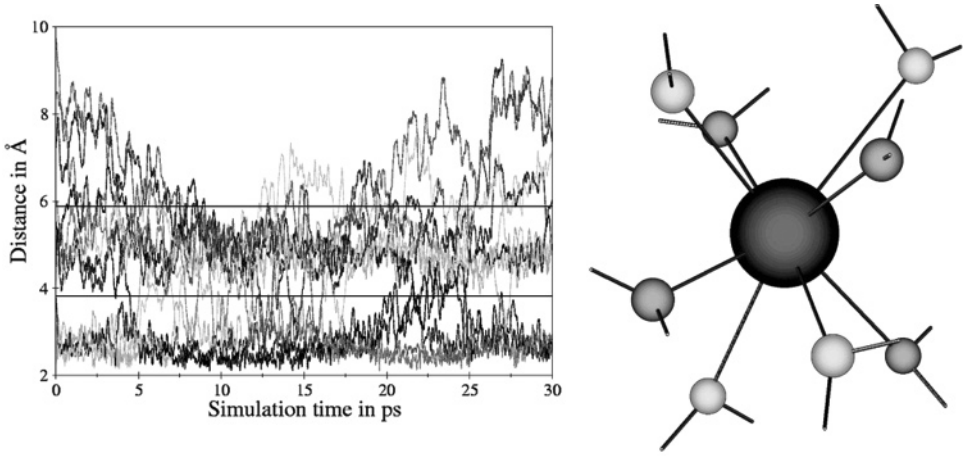

Figure 7. (a) Sn(II)−O distance plot showing water ligand migration between first and second hydration shell. (b) Eight-coordinated Sn(II) ion: exchanging ligands are depicted in pale gray, persistent ligands in dark gray (snapshot taken by MOLVISION).

Table 7. Vibrational and Librational Frequencies in cm^{-1} of First and Second Hydration Shells as Well as Bulk Molecules Obtained from QM/MM MD Simulations of Sn(II) in Aqueous Solution

ion	R_x[a]	R_y	R_z	Q_1[b]	Q_2	Q_3
first shell[c]	460	577	421	3543	1653	3644
second shell	425	573	404	3458	1701	3561
bulk	430	542	417	3451	1699	3556
H_2O (BJH)[d]	420	540	415	3455	1698	3552
H_2O (exp)[e]				3345	1645	3445

[a] R_x, R_y, and R_z denote the librational frequencies of rotation around the three principal axes of the water molecule. [b] Q_1, Q_2, and Q_3 denote the frequencies of the symmetric stretching, bending, and asymmetric stretching vibrations of the water molecule. [c] Ab initio HF frequencies have been scaled by the standard factor 0.89.[33,34] [d] Pure liquid simulation with the BJH water model.[22] [e] Experimental values for liquid water.[43]

Table 8. Mean Ligand Residence Time τ in ps, Number of Accounted Ligand Exchange Events, *N,* and Sustainability of Migration Processes to/from the First and Second Hydration Shell, S_{Ex}

	N^0_{ex}/10 ps[a]	$\tau^0{}_D$[b]	$N^{0.5}_{ex}$/10ps[a]	$\tau^{0.5}{}_D$[b]	S_{ex}[c]	$1/S_{ex}$[d]
first shell	30	2.7	8.0	10.0 (5.0)	0.27	3.8
second shell	496	0.5	63	3.8	0.13	7.9
H_2O[e]	269	0.2	24.0	1.7	0.09	11.2

[a] Number of accounted exchange events per 10 ps lasting at least 0 and 0.5 ps, respectively. [b] MRT determined by the direct method[11] in ps. [c] Sustainability of migration processes. [d] Average number of processes needed for one successful ligand exchange. [e] Values obtained from a QM/MM MD simulation of pure water.[11]

molecules, which is most probably a consequence of the MM treatment of the second shell. The frequencies for the librational motions, R_x, R_y and R_z, obtained from the power spectra of velocity autocorrelation functions (VACFs) using the normal mode approximation[32] are listed in Table 7, and the spectra are displayed in Figure 6. Previous investigations of Ca^{2+},[41] Ni^{2+},[29] Mn^{2+}, and V^{2+} [45] yielded the order $R_y > R_x > R_z$. This order is also detected in the case of hydrated Sn(II), in the first and second hydration shells as well as in the bulk.

Shoulders visible in the peaks of the librational motions of the first shell again indicate the prescence of different species. These shoulders are not visible in the second shell or the bulk. As only rotational movements show signs of these different species while the vibrational motions are unaffected, it can be concluded that steric effects are to be blamed for the occurrence of the different bond lengths rather than an electronic effect such as polarization.

3.2.2. Ligand-Exchange Reactions. The QM/MM MD approach is a suitable tool to characterize ultrafast ligand dynamics as encountered in the case of Sn(II) with its large number of water-exchange processes. Table 8 lists some of the most important dynamical parameters such as the number of ligand-exchange processes, the MRTs, and the sustainability of migration processes between the first and second hydration shells as well as between the second hydration shell and bulk.

During the 30 ps simulation numerous first and second-shell ligand exchanges were observed. The mean ligand residence time (MRT) in pure water (1.7 ps)[11] is much lower than that in the first shell of Sn(II) (10.0 ps) calculated on the basis of the average of eight ligands in the first shell. A detailed analysis of the distance plots revealed that four of the ligands located in the first shell are not exchanging within the simulation time of 30 ps, whereas all other ligands are exchanging frequently between the first and second hydration shells (cf. Figure 7 a). This result is consistent with the data obtained from the Sn−O RDF, the Sn−O spectrum and the rotational spectra identifying two different ligand species within the first shell. The dynamics complete this picture, showing that four ligands are more strongly bound, while all other ligands (four in average) are apparently more weakly bound and thus undergo rapid transitions between first and second hydration shells. Thus, if the average coordination number for the calculation of the MRT is reduced to 4, a MRT value of 5.0 ps would be obtained. The latter value corresponds to very weak solvation and thus to a labile arrangement. The MRT of the first shell of Sn(II) is then considerably lower than those of other divalent ions such as Ca(II),[46] Ba(II),[6] or Hg(II)[5] with MRT values of 42.6, 18.6, and 23.6 ps,[11] respectively, but is on the order of MRTs of monovalent ions such as Rb(I), Cs(I),[4] Ag(I),[40] or Au(I),[39] being 2.0, 1.5, 5.5, and 3.1 ps.[11] The sustainability coefficient S_{ex} of Sn(II) has a value of 0.27, the corresponding $1/S_{ex}$ is 3.8, which means that about four attempts to leave or enter the first hydration shell are needed to achieve one lasting exchange process ($\geq$0.5 ps).

(45) Schwenk, C. F.; Löffler, H. H.; Rode, B. M. *J. Am. Chem. Soc.* **2003**, *125*, 1618.

(46) Schwenk, C. F.; Löffler, H. H.; Rode, B. M. *J. Chem. Phys.* **2001**, *115*, 10808.

In the second shell a total of 1487 border crossings have been registered, 188 of them lasting longer than 0.5 ps. The MRT in the second shell is 3.8 ps. The sustainability coefficient has decreased compared to that of the first shell showing a value of 0.13; its inverse $1/S_{ex}$ is 7.9 which is still lower than that for the pure solvents.

A screenshot of the simulation is depicted in Figure 7b showing an eight-fold square antiprismatic structure of the first shell. The four ligands persisting in the first shell (colored in dark gray) form a distorted tetrahedron. Also, the other ligands (colored in pale gray) form a distorted tetrahedron, showing slightly longer bond distances. Although the system undergoes structural changes when ligands are exchanged during the simulation, similar configurations are being observed throughout the whole trajectory. The antiprismatic structure of the first shell is also reflected by the ADF, showing maxima at 72° and ~139°. The integration of the O−Sn−O distribution indicates that on average four ligands correspond to the smaller angles while three other ligands are associated with larger angles; this reflects the average structural form to be a square antiprism. The tetrahedral substructures found in square prisms are distorted. The broad bandwidth of the ADF peaks as well as the minimum found at 105° points toward a strong internal flexibility of this structure associated with a considerable degree of lability. This lability is well visible from the large number of exchange events observed.

In an early EXAFS and X-ray study Yamaguchi et al.[9] reported three to four ligands stongly bound at 2.25−2.34 Å. Ohtaki reported six ligands surrounding Sn(II) at two different bond lengths. By comparing these data with the results obtained by our QM/MM MD simulation, it can be concluded that the ligands exchanging rapidly between the first and second hydration shells have not been recognized by Yamaguchi et. al. due to the very low MRT. Ohtaki et. al. found two distinct bond lengths but a lower coordination number most probably caused by concentration effects or a too restricted model to fit the spectroscopic data. It could prove worthwhile to reinterpret the measured data on the basis of the structural data supplied by the ab initio QM/MM MD simulation.

4. Conclusion

From the methodical point of view the simulation performed for Sn(II) in aqueous solution confirms that QM/MM MD simulations are a precious tool to investigate the hydration structure of complicated solvate structures, also providing direct access to ultrafast ligand dynamics that are difficult to access by experimental methods.

The simulation has produced a very detailed picture of the Sn(II) hydration structure. A flexible and partly very mobile first hydration shell is on average composed of 8.0 ligands, among which two different types of ligands are present (one binding with a high force constant, the other one showing much weaker bonding) and is thus responsible for the rapid ligand exchange between the first and second hydration shells. The analysis of numerous ligand-exchange reactions yielded mean residence times of 5.0 and 3.8 ps for the first and second hydration shells, respectively.

The observed fast exchange rates suggest the need for a rather sophisticated model to fit spectroscopic data. This model should cover different bond lengths within the first shell, rapid ligand transitions between first and second hydration shells, and a high degree of intershell flexibility. The results of this work could prove helpful for the construction of such a model.

Acknowledgment. Financial support for this work from the Austrian Science Foundation (FWF) is gratefully acknowledged (Project P16221-NO8).

Supporting Information Available: Complete ref 15 and energy expression for the QM/MM MD approach. This material is available free of charge via the Internet at http://pubs.acs.org.

JA052700F